Electrocatalysis (2018) 9:429–436
https://doi.org/10.1007/s12678-018-0457-3

ORIGINAL RESEARCH

Facile Synthesis of Ni-Based Catalysts by Adsorption and Conversion of Metal Ions on Graphene Oxide for Methanol Oxidation

Xihong Guo [1] · Rongli Cui [1] · Huan Huang [1] · Cheng Li [1] · Huanli Yao [1] · Bing Liu [1] · Lele Zhang [1] · Binggang Xu [1] · Jinquan Dong [1] · Baoyun Sun [1]

Abstract

Controllable synthesis of highly dispersed non-precious nanocatalysts is an attractive strategy to prepare efficient electrocatalysts for fuel cell applications. In this study, a facile synthesis of Ni-based mono- and bimetallic nanocatalysts has been developed by adsorption and conversion of metal ions on graphene oxide. The morphology and composition of Ni catalyst are characterized by scanning electron microscopy (SEM), transmission electron microscopy (TEM), X-ray diffraction (XRD), and X-ray photoelectron spectroscopy (XPS). The electrochemical and electrocatalytic properties of Ni catalysts are studied using cyclic voltammetry, chronoamperometry, and electrochemical impedance spectroscopic techniques. The catalytic performance can be improved easily by increasing the adsorption and deposition cycles of metal ions and changing the composition of precursor metal ions solution. This work will be of general interest to design efficient nanostructured catalysts and find ideal electrocatalysts for application with high catalytic performance and low price.

Keywords Electrocatalyst · Graphene oxide · Transition metal · Methanol oxidation · Fuel cells · Nickel

Introduction

Direct methanol fuel cells (DMFCs) have attracted persistent attention among advanced energy conversion technologies due to their high energy density, low pollutant emissions, and simple system configuration [1]. To improve the kinetics of methanol oxidation reaction (MOR), an enormous amount of attention has been focused on the development of efficient electrocatalysts. Typically, in DMFCs, platinum-based catalysts have been extensively used [2]. However, the high cost and the low natural abundance on earth of the Pt-based catalysts severely hamper the practical application of fuel cells [3]. Finding non-precious, active, and durable electrocatalysts to replace Pt for MOR is of critical importance. Transition metals (such as nickel, cobalt, and copper) are very attractive candidates because they are abundant, inexpensive, and efficient electrocatalytic materials. Among them, nickel-based materials have received much attention due to its excellent electrocatalytic performance for the electro-oxidation of methanol demonstrated and long-term stability in alkaline solutions [4–6].

The well-designed catalysts with controllable composition and structure are regarded as a key point to achieve high performance for electrocatalytic applications. It is known that the electrocatalytic activity can be improved significantly when nanostructures are employed [7, 8]. Graphene materials play an important role in constructing nanostructured catalysts due to their high specific surface area, high conductivity, and excellent stability. For instance, graphene materials have attracted great interests as potential catalyst supports in direct methanol fuel cells [9, 10]. Furthermore, the abundant oxygen atoms on the surface of graphene oxide can be used as anchoring sites for metal ions. Graphene materials have been proven to be good adsorbents for metal ions [11]. Although different methods have been used to prepare graphene-supported nanocatalysts, such as chemical precipitation [12], solvothermal methods [13], and microwave irradiation [14], the production of isolated nanoparticles or nanostructures with adjustable composition on the surfaces is still a challenge.

In this work, oppositely charged poly(ethylenimine) (PEI) and GO were first assembled into GO multilayer films via the

---

✉ Baoyun Sun
sunby@ihep.ac.cn

[1] CAS Key Lab for Biomedical Effects of Nanomaterials and Nanosafety, Institute of High Energy Physics, Chinese Academy of Sciences, Beijing 100049, China

spin self-assembly method. Metal ions were spontaneously adsorbed onto the GO films, followed by the conversion of metal ions to metal catalyst in alkaline solution. Various techniques were used to characterize the Ni catalysts, such as scanning electron microscopy (SEM), transmission electron microscopy (TEM), energy dispersive X-ray spectra (EDX), X-ray diffraction (XRD), and X-ray photoelectron spectroscopy (XPS). The electrochemical behavior and electrocatalytic activity of as-prepared metal nanocatalysts were studied. The influence of the adsorption and deposition cycles and the composition of precursor solution were also investigated. Different monometallic or bimetallic catalysts could be prepared using this method.

Experimental

Materials

Poly(ethylenimine) (PEI) was purchased from Alladdin. Natural graphite power (99.9%) was purchased from Qingdao Hensen Graphite Co. Ltd. $NiCl_2$, $CuCl_2$, and $CoCl_2$ were bought from Sinopharm Chemical Reagent Co. Ltd. All other chemicals were obtained from Beijing Chemical Plant. GO was prepared according to a modified Hummer's method using our previously published methods [15]. All the solutions were prepared with Millipore water.

Preparation of Graphene Oxide Films

Prior to coating, ITO (Zhuhai Kaivo Co. Lit, < 15 Ω sq^{-1}, area 0.3 cm^2) was cleaned via sonication in water, ethanol, and acetone sequentially, followed by UV/ozone treatment for 30 min to form negative charges on its surface. The assembly of PEI/GO films was as follows: (1) 20 μL 2 mg mL^{-1} PEI solution was cast onto ITO to completely cover the electrode surface, followed by spinning at the speed of 750 rpm for 5 s and then 5000 rpm for 20 s, and then 20 μL water was cast onto the ITO/PEI surface with the same procedure to wash the surface; (2) step 1 was repeated but with 20 μL GO solution instead of PEI. Then step 1 and step 2 were repeated alternately until forming $(PEI/GO)_3$ films.

Preparation of Ni-Based Catalysts

For Ni deposition, (1) the $(PEI/GO)_3$ films electrodes were immersed in 20 mM $NiCl_2$ for 30 min, followed by twice water washing to remove loosely bounded ions. The water washing process was carried out by dipping the electrodes in 10 mL fresh water for 1 s; (2) a constant potential of −1.0 V was applied to the Ni(II)-loaded electrodes for 120 s in 0.1 M KCl, which had been pre-purged with N_2 for 15 min; (3) after being washed with water, the above electrodes were activated in 0.1 M NaOH by cyclic voltammetry (CV) between 0 to 0.80 V at 100 mV s^{-1} for not less than 50 cycles, until stable cyclic voltammograms were obtained. To increase the loading amount of nickel, the Ni(II) adsorption and deposition procedure could be repeated for several cycles, forming $(PEI/GO)_3$-XNi, where X is the number of Ni(II) adsorption and deposition cycles. As a control, a cleaned ITO was immersed in 20 mM $NiCl_2$ (containing 0.1 M KCl) and the electrode potential was hold at −1.0 V for 120 s, followed by activation in NaOH by CV under the potential range of 0 to 0.80 V at 100 mV s^{-1}. This bulk electrodeposited nickel electrode was named as Ni_{BE} electrode.

For NiCo catalysts preparation, the precursor metal ion solutions were displaced by 20 mM $CoCl_2$ and $NiCl_2$ using direct method. The molar ratios of Ni to Co were 0:100, 50:50, 75:25, and 90:10, forming $(PEI/GO)_3$-XCo, $(PEI/GO)_3$-$XNi_{50}Co_{50}$, $(PEI/GO)_3$-$XNi_{75}Co_{25}$, and $(PEI/GO)_3$-$XNi_{90}Co_{10}$, respectively. For NiCu catalysts preparation, the $(PEI/GO)_3$-XCu, $(PEI/GO)_3$-$XNi_{50}Cu_{50}$, and $(PEI/GO)_3$-$XNi_{90}Cu_{10}$ were prepared using the same method as NiCo.

Characterization and Measurements

A CHI 660D electrochemical workstation was used for electrochemical measurements. A three-electrode cell was used with a saturated calomel electrode (SCE) as the reference electrode, a platinum wire as the counter electrode, and the ITO with films as the working electrode. For MOR, the electrolyte is 0.1 M NaOH and the scan rate is 50 mV s^{-1}. Scanning electron microscopy (SEM) images and energy dispersive X-ray (EDX) spectra were obtained on a Hitachi S4800 with an acceleration voltage of 10 kV. UV-vis experiments were performed with Agilent Cary 5000. Tapping mode atomic force microscope (AFM) image was performed on a Bruker Dimension EDGE. Transmission electron microscopy (TEM) characterization was carried out by JEM-2100Plus. The X-ray diffraction (XRD) data were collected on Bruker D8 Advance diffractometer with Cu Kα radiation. The X-ray photoelectron spectroscopy (XPS) measurements were carried out using an AXIS-Ultra instrument from Kratos Analytical with monochromatic Al Kα radiation ($h\upsilon = 1486.6$ eV).

Results and Discussion

Preparation and Characterization of Ni Catalysts

The scheme of the fabrication of GO films modified electrodes and the procedure of metal ions loading and converting was shown in Fig. 1a. The graphene oxide films were first prepared to deposit Ni catalyst. As shown in Fig. 1b, most GO nanosheets used had heights of ~ 1 nm and length in the range of 200–500 nm. GO is negatively charged in aqueous

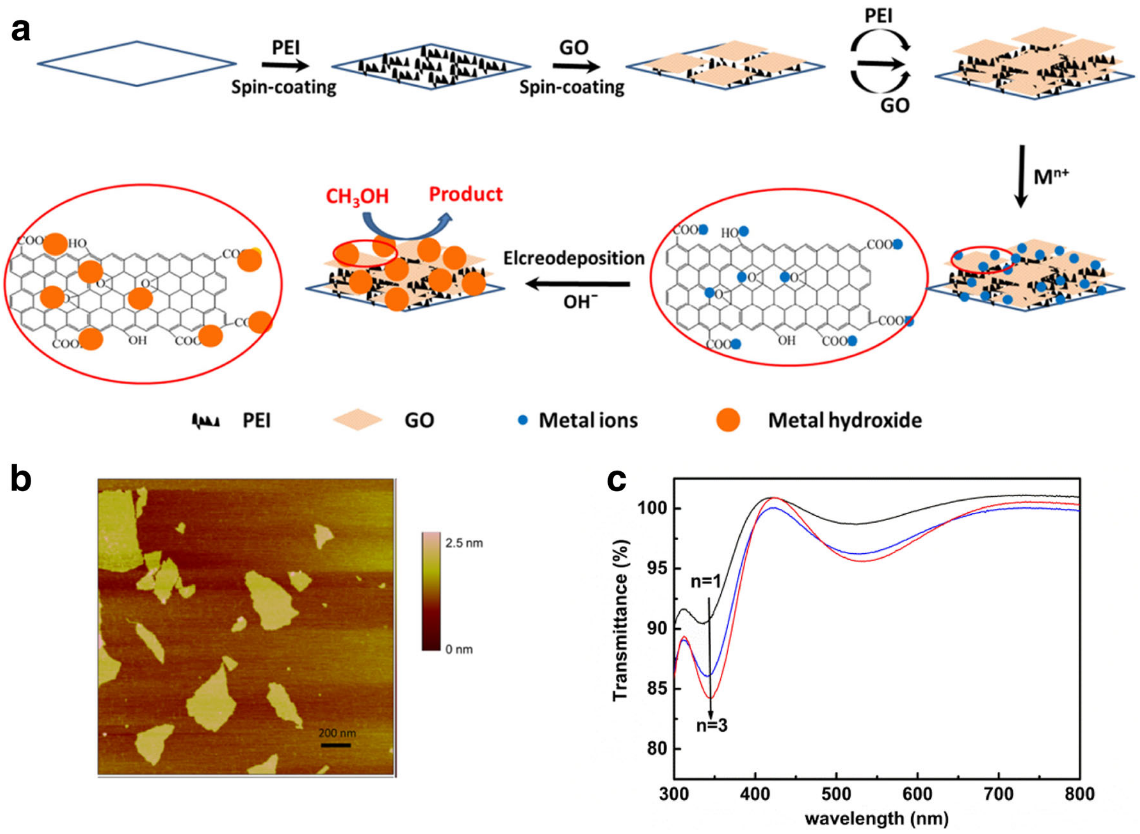

Fig. 1 **a** Scheme of the preparation of Ni-based catalysts for methanol oxidation reaction. **b** AFM image of as-prepared graphene oxide. **c** UV–vis spectra of $(PEI/GO)_n$ ($n = 1, 2, 3$) films assembled on ITO

solution because of its functional groups, such as carboxyl, epoxy, and hydroxyl groups. Thus, positively charged PEI and negatively charged GO were assembled into multilayer films on ITO substrate mainly by electrostatic interaction through spin-coating technique, which is an efficient method for making well-organized multilayer films in a very short process time [16, 17]. The assembly was monitored by UV-vis. The transparency decreased with the assembly numbers (Fig. 1c), which indicated that GO multilayer films were successfully assembled on the surface of ITO.

When the assembled GO films were immersed in $NiCl_2$ solution, Ni(II) would spontaneously diffuse onto the GO surface and bind to negatively charged sites on GO by electrostatic interaction. After the conversion of the Ni(II) ions to metal catalyst, the electrodes were activated in 0.1 M NaOH by CV, which was an important step to create NiOOH compound and initiate the electrochemical activity [18, 19]. During the scanning, a pair of redox peaks appeared in the range 0 to +0.8 V (Fig. 2a). At last, the peaks were stabilized at about 0.55 and 0.42 V, respectively, which was not seen for $(PEI/GO)_3$ films. For comparison, the as-prepared Ni electrode was also scanned in 0.1 M KCl, and no redox peaks were observed (Fig. 2a, inset). The redox peaks should be due to Ni(II)/Ni(III) redox couple with the reaction mechanism shown below [20, 21]:

$$Ni(OH)_2 + OH^- \rightarrow NiOOH + H_2O + e^- \qquad (1)$$

It is inferred that the deposited Ni could be converted to nickel hydroxide as OH^- ions progressively diffused into films. Furthermore, the amount or density of nickel in the films could be controlled by deposition numbers. Upon the transformation of Ni(II), negatively charged sites on GO surface might be regenerated and reused to bind Ni(II). Thus, after one adsorption and deposition cycle, the electrode was immersed in Ni(II) solution again for next loading cycles. As expected, the Ni(II)/Ni(III) redox peaks increased with nickel deposition numbers (Fig. 2b), indicating that the nickel content could be improved easily by repeating the adsorption and deposition cycles.

The formation of Ni catalysts was confirmed by EDX. Nickel peak is observed for $(PEI/GO)_3$-3Ni electrode in EDX spectra (Fig. 3a), indicating the presence of nickel on GO-modified electrode after electrodeposition and activation. TEM was conducted to characterize the morphology and structure of Ni catalysts. These Ni nanocatalysts were randomly decorated onto graphene oxide (Fig. 3b). It was difficult to

Fig. 2 **a** Activated CVs of (PEI/GO)$_3$-1Ni electrode in 0.1 M NaOH solution. **b** CVs of (PEI/GO)$_3$-XNi (X = 0, 1, 2, 3, 4) electrode in 0.1 M NaOH solution

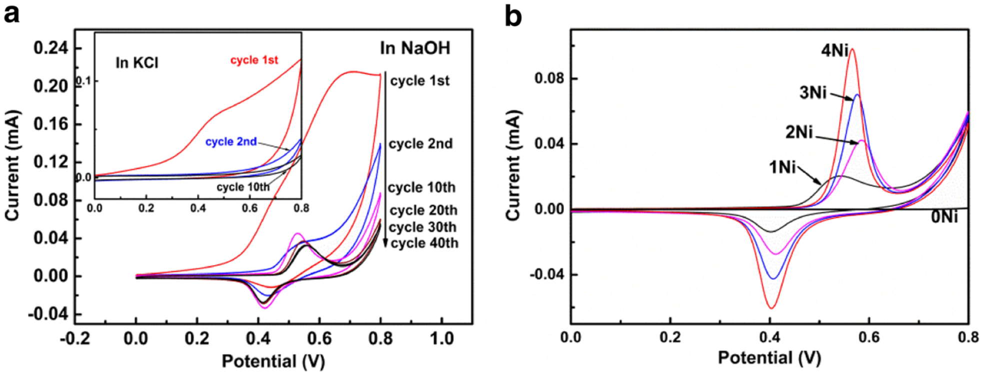

obtain well diffraction peaks by XRD, as the low content and the less crystalline (which could be revealed by TEM). For better comparison, nickel electrode (Ni$_{BE}$) was prepared via bulk electrodeposition from Ni(II) solution to increase the content of Ni, followed by repeated cycling in NaOH. The Ni$_{BE}$ was further characterized by XRD. The XRD pattern of Ni(OH)$_2$ could be observed [22, 23], while some diffraction peaks overlapping with those from the substrate. The chemical composition of the Ni(OH)$_2$ was further provided by XPS. The peaks of the Ni 2p spectrum in Fig. 3d were assigned to the 2p$_{3/2}$ spin orbit levels. And two major peaks and two satellites for Ni 2p$_{3/2}$ and Ni 2p$_{1/2}$ were observed (Ni 2p$_{3/2}$: 855.6 eV, satellite: 861.5 eV, Ni 2p$_{1/2}$: 873.5 eV, satellite: 880.2 eV). This binding energy of the Ni 2p$_{3/2}$ peaks is similar to other instances of Ni(OH)$_2$ and different from that in other reports of NiO (853.7 eV) and Ni (852.6 eV) [24].

Electrochemical and Electrocatalytic Properties of Ni-Based Catalysts

The effect of scan rate on the electrochemical behavior of (PEI/GO)$_3$-XNi electrode was investigated. The cyclic voltammograms of (PEI/GO)$_3$-3Ni electrode in 0.1 M NaOH at different scan rates are represented in Fig. 4a. With increasing the scan rate, the current of Ni(II)/Ni(III) redox couple increased. In addition, the anodic peaks shifted significantly towards more positive potentials and the cathodic peaks shifted slightly towards more negative potentials as the scan

Fig. 3 **a** EDX and SEM (inset) of (PEI/GO)$_3$-3Ni on ITO. **b** TEM image of (PEI/GO)$_3$-3Ni on ITO. **c** XRD patterns of ITO, (PEI/GO)$_3$, (PEI/GO)$_3$-3Ni, and bulk electrodeposited Ni-based catalyst (Ni$_{BE}$). **d** XPS spectrum of (PEI/GO)$_3$-3Ni

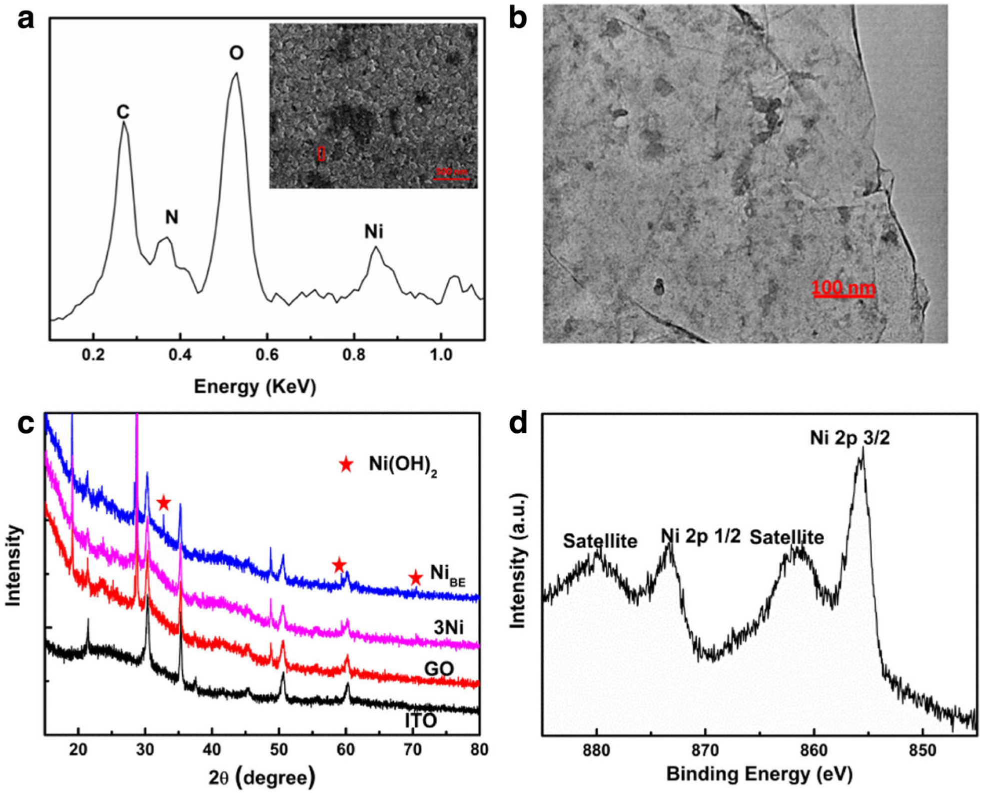

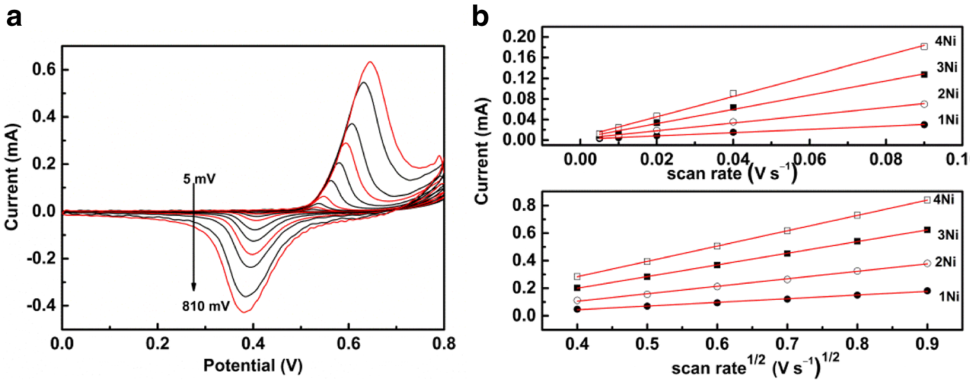

Fig. 4 **a** CVs of (PEI/GO)$_3$-3Ni electrode in 0.1 M NaOH solution at various scan rates (from inner to outer): 5, 10, 20, 40, 90, 160, 250, 360, 490, 640, and 810 mV s^{-1}. **b** The linear dependency of the peak current on the scan rate at lower values (5–90 mV s^{-1}) and the linear dependency of the peak current on the square root of scan rate at higher values (160–810 mV s^{-1})

rate increased. The peak currents were linearly proportional to the scan rate in the range of 5–90 mV s^{-1} (Fig. 4b), suggesting that the electrode reaction of the immobilized Ni(II)/Ni(III) redox couple was a surface-confined electrochemical process. From the slopes of these lines, the surface coverage of the redox species could be calculated using the following equation [25]:

$$I_{\mathrm{p}} = \left(n^2\mathrm{F}^2/4\mathrm{R}T\right)vA\Gamma^* \qquad (2)$$

where Γ^* is the surface coverage of the redox species (mol cm^{-2}) and other symbols have their usual meanings. Taking average of both cathodic and anodic results, Γ^* values were estimated as 1.1×10^{-9} mol cm^{-2} (1Ni), 2.5×10^{-9} mol cm^{-2} (2Ni), 4.5×10^{-9} mol cm^{-2} (3Ni), and 6.4×10^{-9} mol cm^{-2} (4Ni). In the higher scan rates (160–810 mV s^{-1}), the peak currents are linearly proportional to the square root of scan rate (Fig. 4b), signifying the dominance of the diffusion controlled processes. This diffusion process was expressed in Eq. 1 and might occur as a result of the charge neutralization of the film during the oxidation/reduction process [26, 27].

The electrocatalytic activity for MOR of synthesized nickel hydroxide was studied. A significant enhancement in the oxidation current after the complete oxidation of Ni(II) to Ni(III) appeared in the presence of methanol, and the currents increased with the concentration of methanol (Fig. 5a), indicating that the as-synthesized Ni catalysts could promote the oxidation of methanol. The

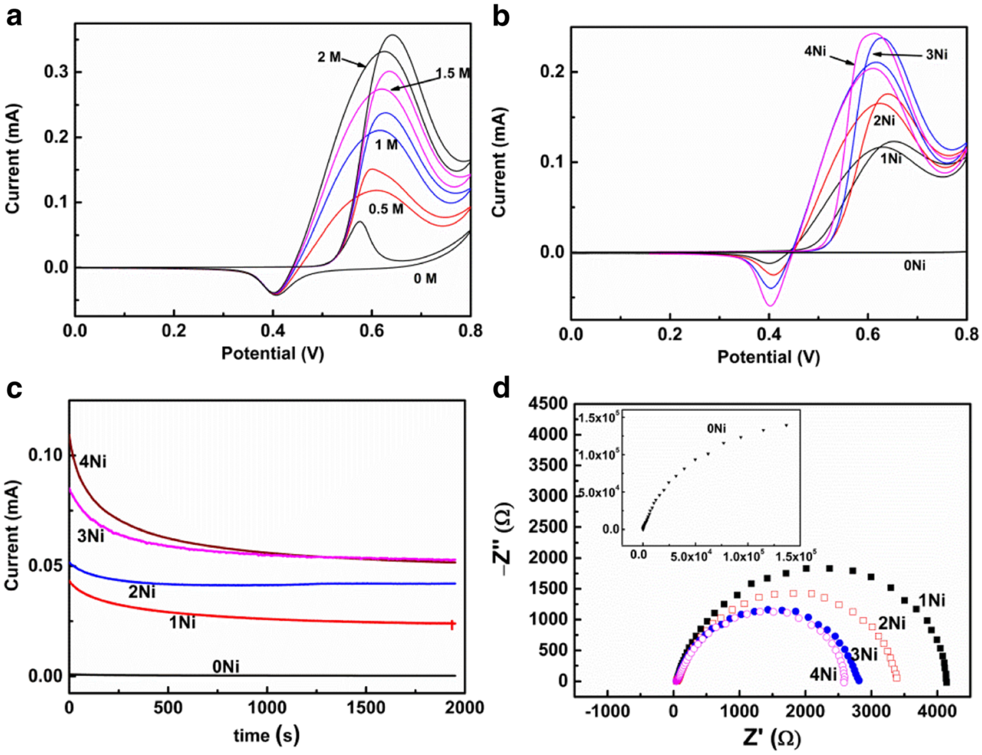

Fig. 5 **a** CVs of (PEI/GO)$_3$-3Ni electrode in 0.1 M NaOH containing different concentration of methanol at scan rate of 50 mV s^{-1}. **b** CVs of (PEI/GO)$_3$-XNi electrode in 0.1 M NaOH containing 1 M methanol at scan rate of 50 mV s^{-1}. **c** Amperometric curves of (PEI/GO)$_3$-XNi electrode in 0.1 M NaOH containing 1 M methanol at 0.65 V. **d** EIS plots of (PEI/GO)$_3$-XNi electrode in 0.1 M NaOH containing 1 M methanol at 0.5 V from 0.1 Hz to 1 × 10^6 Hz. The amplitude of modulation potential was 5 mV

electrochemical oxidation of methanol at nickel or nickel oxide electrodes have been reported and can be represented by the following equation [21]:

$$\mathrm{NiOOH} + \mathrm{methanol} \rightarrow \mathrm{Ni(OH)_2} + \text{oxidation product of methanol} \quad (3)$$

We also investigated the electrocatalytic activity of (PEI/GO)$_3$-XNi electrode for MOR. As shown in Fig. 5b, the catalytic currents increased with the deposition number of Ni (from 0Ni to 4Ni). The electrochemical stability of the (PEI/GO)$_3$-XNi electrodes for methanol oxidation were investigated by chronoamperometry at 0.65 V (Fig. 5c). The currents reached a steady state after a rapid initial decay, indicating a high stability for these Ni catalysts. The catalytic activity of the prepared Ni electrocatalysts for MOR was also studied using electrochemical impedance measurements (EIS), which is an effective tool for studying the interface properties of surface-modified electrodes. The Nyquist impedance plots of (PEI/GO)$_3$-XNi electrode with 1 M methanol in 0.1 M NaOH were shown in Fig. 5d. High frequency semicircle of the Nyquist plots corresponds to the charge transfer resistance. The semicircle diameters decreased with the deposition number of Ni, indicating a faster rate of methanol oxidation at higher Ni content. The presence of Ni greatly decreased the charge transfer resistance for MOR.

As a control, nickel electrode (Ni$_{\mathrm{BE}}$) was prepared via bulk electrodeposition from Ni(II) solution, followed by repeated cycling in NaOH. The enhancement for MOR was also observed on Ni$_{\mathrm{BE}}$ electrode (Fig. 6a, inset). The methanol oxidation peak potential for Ni$_{\mathrm{BE}}$ electrode was around 0.93 V, which was much more positive than that for (PEI/GO)$_3$-XNi electrode (Fig. 5b). For better comparison, currents were also normalized by the mass of electroactive Ni(OH)$_2$ ($m_{\mathrm{Ni(OH)2}}$), to provide a value for specific activity (current/mass = A $\mathrm{g_{Ni(OH)2}}^{-1}$) [28, 29]:

$$\text{specific activity} = i/m_{\mathrm{Ni(OH)2}}, \text{ where } m_{\mathrm{Ni(OH)2}} = \Gamma^{*} \times M_{\mathrm{Ni(OH)2}} \quad (4)$$

The (PEI/GO)$_3$-3Ni electrode showed enhanced mass-normalized activity for the MOR relative to Ni$_{\mathrm{BE}}$ electrode (Fig. 6a). These results indicated that the Ni catalysts by adsorption and deposition of Ni(II) were much more active for methanol oxidation. Obviously, the high activity was mainly due to the contribution of graphene oxide. As the precursor metal ions were located around the negatively charged sites of GO, the GO films probably inhibited the aggregation of nanocomposites, which would increase the amount of electroactive sites. To support the above speculation, the morphology of Ni$_{\mathrm{BE}}$ electrode was further investigated by SEM. Large agglomerates were observed on the surface from SEM image (Fig. 6b). While the transmittance of the (PEI/GO)$_3$-3Ni electrode was above 80%, the transmittance of the Ni$_{\mathrm{BE}}$ electrode was close to 0%, indicating a dense Ni film was presumably formed by bulk electrodeposition in Ni(II) solution. From the above, it was speculated that isolated and nanostructured catalysts were obtained by adsorption and deposition of Ni(II) adsorbed onto GO with high activity.

Preparation of Ni-Based Bimetallic Catalysts

Besides nickel, other transition mono- or bimetallic catalysts were prepared by changing the precursor solution using this method. As shown in Fig. 7a, the obtained Co-based catalysts promoted the methanol oxidation reaction but with lower catalytic activity for MOR. The presence of Ni in Co-based catalysts significantly improved the oxidation currents for MOR (Fig. 7b). Moreover, the onset potential of methanol oxidation was 0.30 V ((PEI/GO)$_3$-3Co), 0.48 V ((PEI/GO)$_3$-3Ni$_{50}$Co$_{50}$), 0.50 V ((PEI/GO)$_3$-3Ni$_{75}$Co$_{25}$), 0.52 V ((PEI/GO)$_3$-3Ni$_{90}$Co$_{10}$), and 0.57 V ((PEI/GO)$_3$-3Ni), respectively. The addition of Co decreased the overpotential for the methanol oxidation. Figure 6b (inset) showed the cyclic voltammograms for pure Co, pure Ni, and mixed Ni/Co hydroxides. The redox peaks were also shifted to less positive potentials in the presence of Co, indicating the doping of Co can facilitate the redox processes of Ni(II)/Ni(III). It was agreed with previous reports that the incorporation of Co into nickel catalysts can increase the

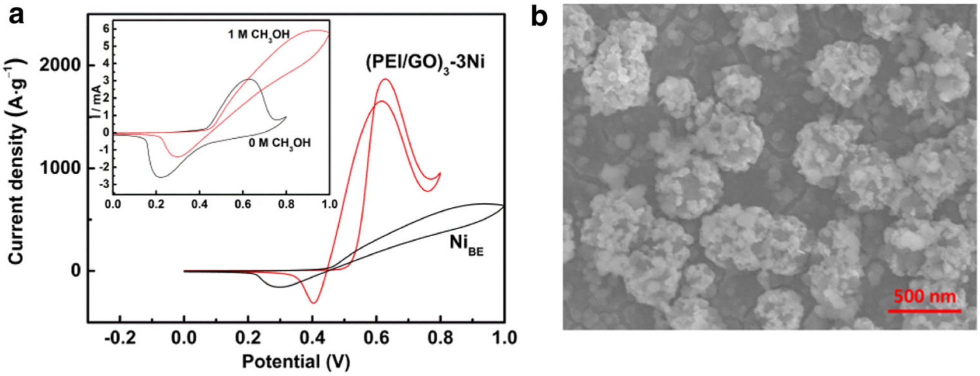

Fig. 6 **a** CVs of the (PEI/GO)$_3$-3Ni and Ni$_{\mathrm{BE}}$ electrode in 0.1 M NaOH containing 1 M methanol. Inset: CVs of the Ni$_{\mathrm{BE}}$ electrode in 0.1 M NaOH containing 0 and 1 M methanol. **b** SEM image of the Ni$_{\mathrm{BE}}$ film on ITO

Fig. 7 **a** CVs of (PEI/GO)$_3$-3Co electrode in 0.1 M NaOH containing 0, 0.2, 0.5, 1, 1.5, and 2 M methanol. **b** CVs of (PEI/GO)$_3$-3Ni, (PEI/GO)$_3$-3Ni$_{50}$Co$_{50}$, (PEI/GO)$_3$-3Ni$_{75}$Co$_{25}$, (PEI/GO)$_3$-3Ni$_{90}$Co$_{10}$, and (PEI/GO)$_3$-3Co electrode in 0.1 M NaOH containing 0 (inset) and 0.5 M methanol. **c** CVs of (PEI/GO)$_3$-3Cu electrode in 0.1 M NaOH containing 0, 0.2, 0.5, 1, 1.5, and 2 M methanol. **d** CVs of (PEI/GO)$_3$-3Ni, (PEI/GO)$_3$-3Ni$_{50}$Cu$_{50}$, (PEI/GO)$_3$-3Ni$_{75}$Cu$_{25}$, (PEI/GO)$_3$-3Ni$_{90}$Cu$_{10}$, and (PEI/GO)$_3$-3Cu electrode in 0.1 M NaOH containing 0 (inset) and 0.5 M methanol

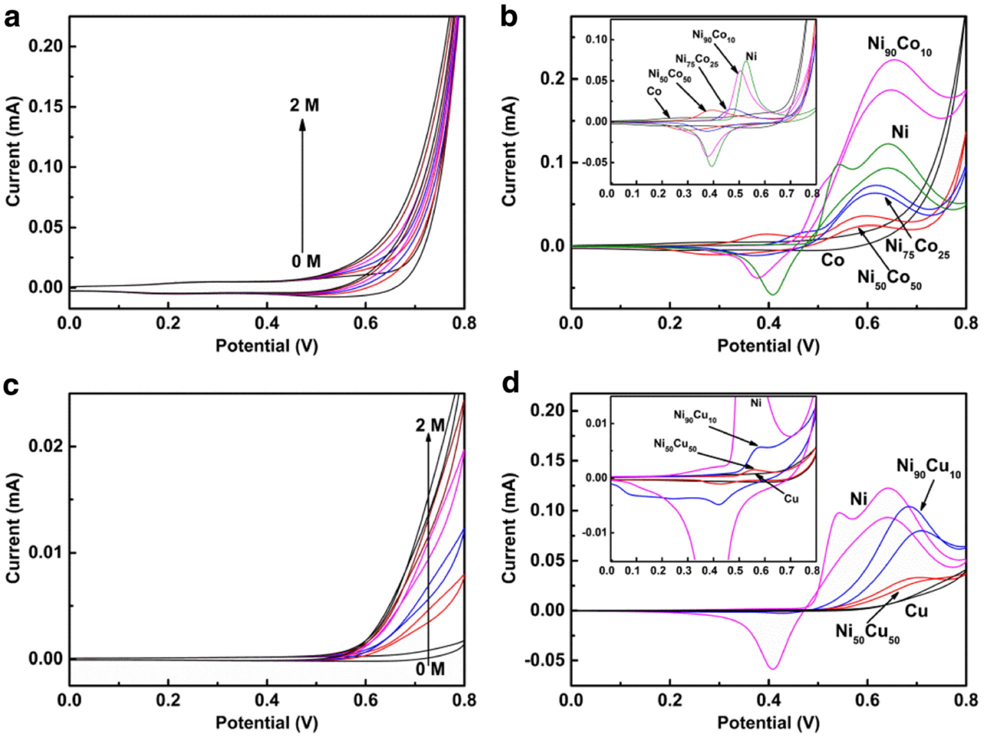

activity for MOR [30]. We also prepared Cu and NiCu composites using the method of the adsorption and deposition metal ions. The as-prepared monometallic or bimetallic catalysts also exhibited enhancement for MOR (Fig. 7c, d). Unlike Co, the addition of Cu increased the overpotential for the methanol oxidation. As a result, this method can be used to prepare different single or mixed metallic composites for catalytic applications. Furthermore, the catalytic activity can be controlled by simply changing the composition of precursor solution.

Conclusions

In this work, we have developed a new method for the preparation of mono- and bimetallic catalysts by direct adsorption and deposition of metal ions adsorbed on GO films. As the precursor metal ions are located around the negatively charged sites of GO, isolated and nanostructured catalysts are obtained after the transformation of Ni(II). The as-synthesized Ni nanocatalysts have shown good electrocatalytic activity and stability for methanol oxidation. The catalytic performance is improved simply by increasing the adsorption and deposition cycles to increase the nickel loading content. Furthermore, various monometallic or bimetallic catalysts can be prepared using this strategy. The catalytic activity can be controlled by the composition of precursor solution. Such findings will provide an innovative way to design efficient non-precious catalysts and find ideal electrocatalysts for fuel cells with high catalytic performance and low price.

Funding This work was supported by the National Basic Research Program of China (2016YFA0203200) and the National Natural Science Foundation of China (U1632113, 11705211, 21402202, and 11505191).

References

1. M.M. Liu, R.Z. Zhang, W. Chen, Graphene-supported nanoelectrocatalysts for fuel cells: Synthesis, properties, and applications. Chem. Rev. **114**, 5117 (2014)
2. A.C. Chen, P. Holt-Hindle, Platinum-based nanostructured materials: Synthesis, properties, and applications. Chem. Rev. **110**, 3767 (2010)
3. D.J. Chen, Y.Y.J. Tong, Irrelevance of carbon monoxide poisoning in the methanol oxidation reaction on a PtRu electrocatalyst. Angew. Chem. Int. Ed. **54**, 9394 (2015)
4. S. De, J.G. Zhang, R. Luque, N. Yan, Ni-based bimetallic heterogeneous catalysts for energy and environmental applications. Energy Environ. Sci. **9**, 3314 (2016)
5. R.M.A. Tehrani, S. Ab Ghani, The nanocrystalline nickel with catalytic properties on methanol oxidation in alkaline medium. Fuel Cells **9**, 579 (2009)
6. M. Guo, Y. Yu, J. Hu, Nickel nanoparticles for the efficient electrocatalytic oxidation of methanol in an alkaline medium. Electrocatalysis **8**, 392 (2017)
7. A.S. Arico, P. Bruce, B. Scrosati, J.M. Tarascon, V.W. Schalkwijk, Nanostructured materials for advanced energy conversion and storage devices. Nat. Mater. **4**, 366 (2005)

8. X.Q. Zhang, X.B. Cheng, Q. Zhang, Nanostructured energy materials for electrochemical energy conversion and storage: A review. J. Energy Chem. **25**, 967 (2016)
9. X.B. Fan, G.L. Zhang, F.B. Zhang, Multiple roles of graphene in heterogeneous catalysis. Chem. Soc. Rev. **44**, 3023 (2015)
10. N. Seselj, C. Engelbrekt, J.D. Zhang, Graphene-supported platinum catalysts for fuel cells. Sci. Bull. **60**, 864 (2015)
11. F. Perreault, A.F. de Faria, M. Elimelech, Environmental applications of graphene-based nanomaterials. Chem. Soc. Rev. **44**, 5861 (2015)
12. W.J. Huang, H.T. Wang, J.G. Zhou, J. Wang, P.N. Duchesne, D. Muir, P. Zhang, N. Han, F.P. Zhao, M. Zeng, J. Zhong, C.H. Jin, Y.G. Li, S.T. Lee, H.J. Dai, Highly active and durable methanol oxidation electrocatalyst based on the synergy of platinum-nickel hydroxide-graphene. Nat. Commun. **6** (2015)
13. A.K. Das, R.K. Layek, N.H. Kim, D. Jung, J.H. Lee, Reduced graphene oxide (RGO)-supported $NiCo_2O_4$ nanoparticles: An electrocatalyst for methanol oxidation. Nanoscale **6**, 10657 (2014)
14. Z.G. Wang, Y. Hu, W.L. Yang, M.J. Zhou, X. Hu, Facile one-step microwave-assisted route towards Ni nanospheres/reduced graphene oxide hybrids for non-enzymatic glucose sensing. Sensors **12**, 4860 (2012)
15. R.L. Cui, J. Li, H. Huang, M.Y. Zhang, X.H. Guo, Y.A. Chang, M. Li, J.Q. Dong, B.Y. Sun, G.M. Xing, Novel carbon nanohybrids as highly efficient magnetic resonance imaging contrast agents. Nano Res. **8**, 1259 (2015)
16. J. Cho, K. Char, J.D. Hong, K.B. Lee, Fabrication of highly ordered multilayer films using a spin self-assembly method. Adv. Mater. **13**, 1076 (2001)
17. S. Song, H. Liu, X. Guo, N. Hu, Comparative electrochemical study of myoglobin loaded in different polyelectrolyte layer-by-layer films assembled by spin-coating. Electrochim. Acta **54**, 5851 (2009)
18. N.A.M. Barakat, M. Motlak, A.A. Elzatahry, K.A. Khalil, E.A.M. Abdelghani, Ni_xCo_{1-x} alloy nanoparticle-doped carbon nanofibers as effective non-precious catalyst for ethanol oxidation. Int. J. Hydrog. Energy **39**, 305 (2014)
19. X. Cui, W.L. Guo, M. Zhou, Y. Yang, Y.H. Li, P. Xiao, Y.H. Zhang, X.X. Zhang, Promoting effect of Co in Ni_mCo_n $(m + n = 4)$ bimetallic electrocatalysts for methanol oxidation reaction. ACS Appl. Mater. Interfaces **7**, 493 (2015)
20. A.A. El-Shafei, Electrocatalytic oxidation of methanol at a nickel hydroxide/glassy carbon modified electrode in alkaline medium. J. Electroanal. Chem. **471**, 89 (1999)
21. M.A.A. Rahim, R.M.A. Hameed, M.W. Khalil, Nickel as a catalyst for the electro-oxidation of methanol in alkaline medium. J. Power Sources **134**, 160 (2004)
22. L.L. Zhang, Z.G. Xiong, X.S. Zhao, A composite electrode consisting of nickel hydroxide, carbon nanotubes, and reduced graphene oxide with an ultrahigh electrocapacitance. J. Power Sources **222**, 326 (2013)
23. H.L. Wang, H.S. Casalongue, Y.Y. Liang, H.J. Dai, $Ni(OH)_2$ nanoplates grown on graphene as advanced electrochemical pseudocapacitor materials. J. Am. Chem. Soc. **132**, 7472 (2010)
24. J.W. Lee, T. Ahn, D. Soundararajan, J.M. Ko, J.D. Kim, Non-aqueous approach to the preparation of reduced graphene oxide/α-$Ni(OH)_2$ hybrid composites and their high capacitance behavior. Chem. Commun. **47**, 6305 (2011)
25. A.J. Bard, L.R. Faulkner, *Electrochemical methods: Fundamentals and applications*, second edn. (John Wiley & Sons, Inc., New York, 2001)
26. L. Zheng, J.F. Song, Electrocatalytic oxidation of methanol and other short chain aliphatic alcohols at Ni(II)-quercetin complex modified multi-wall carbon nanotube paste electrode. J. Solid State Electrochem. **14**, 43 (2010)
27. W. Wang, R. Li, X. Hua, R. Zhang, Methanol electrooxidation on glassy carbon electrode modified with bimetallic Ni(II)Co(II)salen complexes encapsulated in mesoporous zeolite A. Electrochim. Acta **163**, 48 (2015)
28. L.A. Hutton, M. Vidotti, A.N. Patel, M.E. Newton, P.R. Unwin, J.V. Macpherson, Electrodeposition of nickel hydroxide nanoparticles on boron-doped diamond electrodes for oxidative electrocatalysis. J. Phys. Chem. C **115**, 1649 (2011)
29. P.E. Sharel, D.Q. Liu, R.A. Lazenby, J. Sloan, M. Vidotti, P.R. Unwin, J.V. Macpherson, Electrodeposition of nickel hydroxide nanoparticles on carbon nanotube electrodes: Correlation of particle crystallography with electrocatalytic properties. J. Phys. Chem. C **120**, 16059 (2016)
30. Y.Y. Tong, C.D. Gu, J.L. Zhang, H. Tang, Y. Li, X.L. Wang, J.P. Tu, Urchin-like Ni-Co-P-O nanocomposite as novel methanol electro-oxidation materials in alkaline environment. Electrochim. Acta **187**, 11 (2016)